PHYSICAL REVIEW B **79**, 245313 (2009)

Terahertz acoustic oscillations by stimulated phonon emission in an optically pumped superlattice

P. M. Walker, A. J. Kent, and M. Henini
School of Physics and Astronomy, University of Nottingham, University Park, Nottingham NG7 2RD, United Kingdom

B. A. Glavin, V. A. Kochelap, and T. L. Linnik
V E Lashkarev Institute of Semiconductor Physics, Pr. Nauki 41, Kiev 03028, Ukraine
(Received 9 February 2009; published 17 June 2009)

A source of nanometer wavelength, transverse-polarized, sound waves based on stimulated emission of phonons in a semiconductor superlattice inside an acoustic cavity and pumped by a low-average power nanosecond pulsed laser is described. The experimental evidence for sound laser (saser) action in our device is a superlinear increase in emitted acoustic intensity and an increase in emission directionality above a threshold in the peak optical pumping power at ~ 500 W cm^{-2}. We also show that saser action is theoretically possible in the device due to strong electron-phonon coupling, the achievement of population inversion under optical pumping and effective phonon confinement in an acoustic cavity.

DOI: 10.1103/PhysRevB.79.245313 PACS number(s): 63.20.D−, 63.22.Np, 73.63.Hs

I. INTRODUCTION

In recent years, there has been a rapid growth in interest in developing techniques for the generation and detection of nanometer-wavelength sound in solids. In typical solids, with the speed of sound a few thousand meters per second, this means a sound frequency of order a terahertz (10^{12} Hz). Such high-frequency sound waves are a useful tool for studying embedded nanostructures and would complement other nanometrology techniques such as atomic force microscopy, scanning tunnel microscopy, and TEM which probe surfaces or require destructive processing of the sample. An example is the use of nonequilibrium phonons to probe embedded quantum dots.[1] However, the work described in Ref. 1 used incoherent phonons with a broad, Planck, frequency spectrum. Application of acoustics to the study of nanostructures would benefit from access to a source of coherent nanometer-wavelength sound. Such sources of coherent terahertz sound have been demonstrated (see, e.g., Refs. 2–7 and references therein) but these require the use of specialized equipment including expensive femtosecond pulsed laser systems. A device which is the acoustic equivalent of an optical laser, e.g., a saser [for: sound amplification by stimulated emission of (acoustic) radiation], would emit an intense beam of coherent sound under electrical or optical pumping, and could potentially transform the field of terahertz acoustics, just as the laser has transformed optical spectroscopy and imaging.

The operation of lasers is based on the fundamental phenomenon of stimulated emission in systems having a population inversion. Stimulated emission is not restricted to photons, it is possible for any elementary excitation obeying bosonic statistics. In solids, for example, stimulated emission is demonstrated for photons, plasmons[8] and optical phonons.[9] For high-frequency acoustic phonons, the theoretical possibility of sound amplification by stimulated emission of radiation has been discussed in the scientific literature; see for example Refs. 10–12. Practical demonstrations of stimulated emission of acoustic phonons are few, and include the case of inversely populated impurity states subject to very strong optical pumping and for acoustic frequency up to only about 50 GHz corresponding to a wavelength of about 200 nm (see Ref. 13 and references therein). Recently, stimulated emission of terahertz longitudinal-polarized acoustic phonons from GaAs/AlAs superlattices (SLs) under hopping electron transport has been demonstrated.[14] In that case the population inversion was created between the Stark levels under electrical bias.

A large class of contemporary semiconductor laser devices is based on heterostructures having nanoscale feature sizes, which present many opportunities to engineer the electronic states and provide strong population inversion under pumping. When considering the possibility of a saser, it is necessary to take account of the fact that, in crystals, the speed of sound is about 5 orders of magnitude less than the speed of light. As a result, for a given frequency, acoustic phonons have a much shorter wavelength than photons. In particular, for the terahertz frequency band, the wavelength is only a few nanometers. This suggests that for a heterostructure-based saser not only the electron states, but also the phonon states and their coupling with electrons can be tailored to facilitate its operation. On the other hand, the short wavelength of terahertz sound as well as its relatively strong scattering in comparison to light[15] brings about severe requirements for design of the acoustic cavity. It has been demonstrated, however, that modern epitaxial growth technologies enable the production of high-quality acoustic cavities for terahertz frequencies.[16]

Here we present evidence of saser action for transverse (shear) acoustic modes at 500 GHz in an optically pumped semiconductor SL without applied electrical bias. The device exploits the effect of strong enhancement of the piezoelectric electron-phonon interaction in SLs.[17] The enhancement is due to "resonance" of the acoustic wavelength with the periodicity of the piezoelectric coupling constant in the SL, and occurs only for transverse-polarized phonons, propagating very close to the SL growth axis and having energy $\hbar\omega = 2\pi n\hbar c_s/d$ where d is the repeat period of the SL, c_s the velocity of sound and n is an integer. One might expect such an enhanced interaction to facilitate transfer of the system into the regime of stimulated emission.

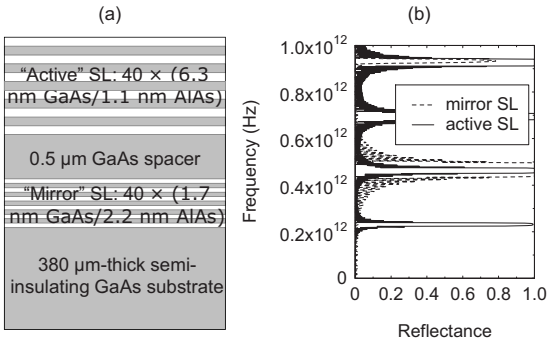

FIG. 1. (a) Structure of the optically pumped saser device; (b) calculated frequency-dependence of the reflectivity of the Bragg mirror and active superlattices for transverse-polarized sound.

The structure of the paper is the following: in Sec. II we describe the devices under investigation and the experimental system. The results of measurements suggesting stimulated character of phonon emission in our system are presented in Sec. III. In Sec. IV we present a theoretical analysis explaining the observed behavior.

II. DETAILS OF EXPERIMENT

The structure of the experimental device is shown in Fig. 1. It was grown by molecular-beam epitaxy on a 0.38-mm-thick semi-insulating GaAs substrate. From top to the bottom, the structure consists of: a 40-period GaAs/AlAs SL (which we will call the active SL) with the quantum well (QW) and barrier layer thickness $d_{QW}=6.3$ nm, and $d_B=1.1$ nm; a 0.5-μm-thick GaAs spacer; and another 40-period GaAs/AlAs SL (the mirror SL) with the GaAs and AlAs layer thickness of 1.7 and 2.2 nm, respectively.

Due to the different acoustic impedances of GaAs and AlAs, sound is partially reflected at the heterointerfaces. Bragg reflection of sound occurs at wavelengths $2d_M/n$, where n is an integer and d_M is the mirror SL period ($d_M=3.9$ nm). The parameters of the active and mirror SLs were selected such that the phonons in the spectral band for which the piezoelectric electron-phonon interaction is enhanced in the active SL are also strongly reflected by the mirror SL (see Fig. 1). Thus, the phonons are confined in the Fabry-Pérot cavity between the sample surface, which acts as a mirror,[18] and the SL Bragg mirror. In addition to the structure shown in Fig. 1, we also produced a control structure which was the same, except that it had no mirror SL.

The experimental setup is illustrated in Fig. 2. The active SL was subject to interband optical excitation by a tunable CW Ti:sapphire laser focused to a spot of about 50 μm diameter on the sample surface It should be noted that the presence of the relatively thick GaAs spacer between the active SL and mirror SL prevents light absorption in the latter. The laser beam was chopped by an acousto-optic modulator to produce pulses of duration about 30 ns. The acoustic emission from the structure was detected using a superconducting aluminum bolometer fabricated on the surface of the GaAs substrate opposite the SL structure. The measurements were performed at temperature of about 2 K, on the bolometer superconducting transition. At this low temperature, most of the terahertz acoustic phonons reach the bolometer ballistically with no scattering. The longitudinal and transverse-polarized phonons travel at different speeds and so can be discriminated by their different arrival time. A typical bolometer signal is also shown in Fig. 2. The onset of the signal occurs about 130 ns after the laser pulse is incident on the sample, which corresponds to the ballistic time of flight of low-frequency (<1 THz) transverse-polarized acoustic phonons in the substrate. Very little signal is detected at the expected arrival time for longitudinally polarized phonons (~80 ns, not seen on the scale of Fig. 2). The peak in the signal at about 190 ns is followed by a slowly decaying tail which is normally attributed to quasidiffusive propagation of the acoustic phonon decay products of emitted optical phonons.

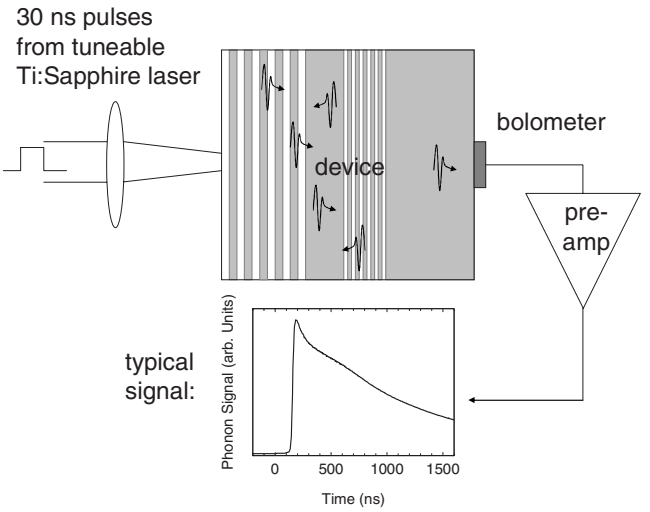

FIG. 2. Experimental arrangement, showing a typical time-resolved bolometer trace. The onset of the bolometer signal is about 120 ns after the laser pulse hits the sample.

III. EXPERIMENTAL SIGNATURES OF STIMULATED PHONON EMISSION

The results of measurements of the peak intensity of the transverse-acoustic phonon signal as a function of pumping power density are shown in Fig. 3(a), for the case when the excitation laser spot is aligned on the part of the SL directly opposite the bolometer and for two values of the laser excitation wavelength, 720 and 750 nm (these values correspond to the photon energy exceeding the effective band gap of the SL by about 100 and 30 meV, respectively). The most important feature is the threshold observed at a pumping power density of about 500 W cm^{-2}. No such threshold is observed if the laser photon energy is below the fundamental band gap in the active SL or if the laser spot is not positioned directly opposite the bolometer. By analogy with measurements on optical laser structures, the pumping threshold suggests the stimulated character of the transverse-acoustic phonon emission.

Figure 4(a) shows the bolometer signals for a pump power density of 1650 W cm^{-2} and photon energies both

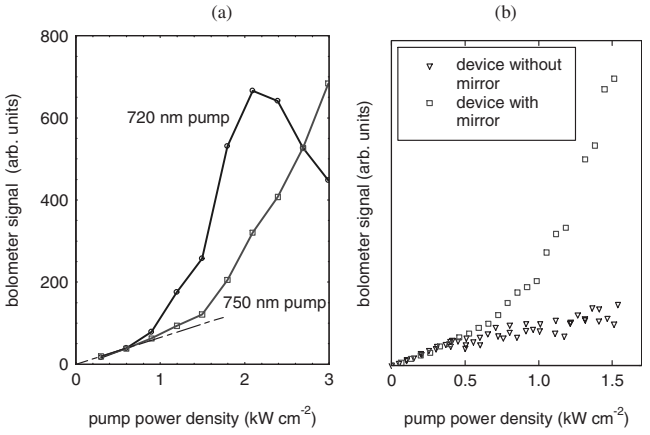

FIG. 3. (a) Bolometer signal as a function of the pump power-density incident on the sample for two different pump wavelengths, 720 and 750 nm. (b) Detail of the region close to the threshold for 750 nm wavelength pump, and, for comparison, the pump power-density dependence of the signal for the sample without an acoustic Bragg mirror.

below and above the SL fundamental band gap. There is a clear difference between the signals in the first 130–180 ns where the signal is strongly enhanced when the photon energy is larger than the gap. As both photon energies are well above the bulk GaAs band gap, we conclude that the change in the nature of the signal must be due to optical excitation of the SL which emits largely low-frequency acoustic phonons. Similarly, as shown in Fig. 4(b), for photon energy larger than the gap, the dependence of the signal on pump power density shows a significant increase in the low-frequency acoustic phonon component when the pump power density is increased above the threshold value. Note that in Fig. 4(b) the signals have been normalized to the pump power so that the change in shape of the pulse is not masked by the large overall increase in intensity. The signals shown in Fig. 4 were all recorded with the pump spot positioned directly opposite the bolometer. The dependences of the signal on pump photon energy and power were very much weaker if the pump spot was moved so that it did not overlap with the active area of the bolometer.

Previous measurements of the phonon emission by optically excited bulk GaAs (Ref. 19) also showed a superlinear increase in the ballistic low-frequency acoustic phonons with increasing excitation power density above a few hundred W cm^{-2}. The authors attributed this to the formation of a dense electron-hole plasma at high optical power density. Rapid intercarrier scattering within the plasma and acoustic phonon emission bypasses the optical phonon emission channel which dominates at much smaller excitation power densities. There are some important differences between the measurements described here and in Ref. 19: in our case, optical pumping of a SL is taking place, and the pump photon energy is at the most only a few units of the optic phonon energy above the effective band gap. However, stronger evidence that the observed threshold is probably due to stimulated phonon emission and not the process described in Ref. 19, was obtained by performing the same measurements on the control sample having no mirror SL. The mirror SL does

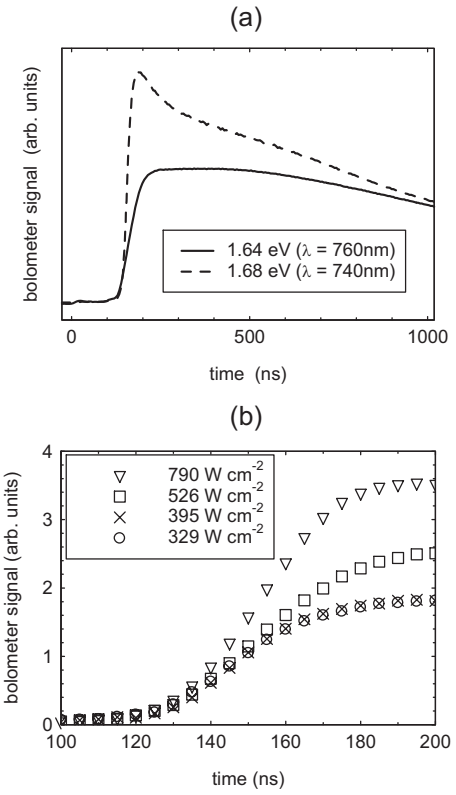

FIG. 4. Phonon signals for the pump spot directly opposite the bolometer: (a) comparison of the bolometer signals at two different pump photon energies, corresponding to below and above the fundamental band gap of the SL, and for constant power density of 1650 W cm^{-2}; (b) comparison of the bolometer signals in the temporal range corresponding to the arrival of low-frequency transverse-acoustic phonons at four different pump power densities, two below and two above the threshold level. The signals have been normalized to the power density and were taken at a pump wavelength of 750 nm.

not influence the propagation of sound of frequency outside the narrow bands where Bragg reflection occurs. Therefore, if the process described in Ref. 19 was responsible for the observed threshold, then we should expect to observe it using both samples. The detailed dependences up to 1500 W cm^{-2} for both samples pumped at $\lambda = 750$ nm are shown in Fig. 3(b). There is clearly no threshold seen for the sample without the mirror SL, which means that stimulated emission of phonons, combined with their accumulation in the Fabry-Pérot acoustic cavity, is the more likely explanation for the above-threshold enhancement of the phonon emission in the sample with an acoustic mirror SL.

Additional experimental evidence for stimulated phonon emission and saser action of the structure is the more directional character of sound emission above the threshold. We have already pointed out that the threshold and enhancement of the ballistic transverse-acoustic phonon signal is only observed when the pump-laser spot is directly opposite the bolometer. Here we make measurements of the spatial dependence of the ballistic phonon intensity using the phonon imaging technique,[20] where the excitation laser spot is scanned over the surface of the SL opposite to the bolometer.

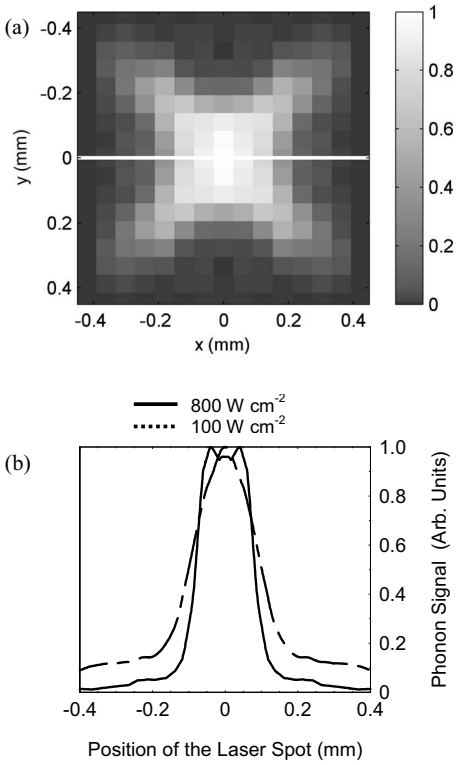

FIG. 5. (a) Image of the bolometer signal intensity as a function of the pump spot displacement. The position (0; 0) corresponds to the pump spot directly opposite the bolometer. The horizontal line through the centre of the image indicates the y position of the above and below-threshold line scans shown in (b). For clarity, the line scans have each been normalized to their peak.

Fig. 5 shows an image of the emission from the structure with a mirror SL and line scans of the acoustic intensity at pump powers corresponding to below and above threshold. It is clear that as the pump power is increased above the threshold, the angular width of the emission reduces. For below-threshold pumping, the spatial distribution of the phonon flux is as expected for TA phonon focusing in the cubic GaAs substrate,[20] but broadened to allow for the finite size of the laser spot and bolometer. Above threshold, the observed spatial distribution can be quantitatively accounted for by the overlap of the laser spot with the bolometer, with only a small correction due to phonon focusing effects. This suggests that, when pumping above threshold, the emitted phonon wave vectors are in a direction very close to the normal to the SL layers. On the other hand, for the sample without the mirror SL, increasing the pumping gave rise to a small angular broadening of the emission. This is to be expected since, in the absence of sasing, pumping at higher power would normally result in the emission of higher energy phonons which will be more strongly scattered on their way to the bolometer.

We claim that the observation of the pumping threshold and concomitant narrowing of the angular range of the acoustic emission provide compelling experimental evidence for stimulated emission and sasing in the structure with a Bragg mirror SL. This is also supported by the absence of both a threshold and increased directionality in the control sample which has no acoustic cavity.

IV. THEORY OF THE ACOUSTIC PHONON POPULATION INSTABILITY

In this section we go on to show that these experimental observations are consistent with a theoretical model of the electron inversion and phonon amplification produced in the active SL by optical pumping. Pumping of the active SL with interband light having photon energy greater than the effective band gap, E_g^*, leads to the creation of nonequilibrium photoexcited electrons and holes in the QWs. In isolated QWs, the initial nonequilibrium electron distribution will relax to the bottom of the band and, due to fast scattering, inversion is lost. However, because the AlAs barrier layers of the active SL are sufficiently narrow, electrons are able to tunnel through them and an extended electron miniband is formed.[21] This ensures fast escape of nonequilibrium electrons from the SL and so maintains the inversion electron distribution produced by the optical pumping. The escape time is determined by the length of the active SL and the electron velocity. For the active SL used in our experiments, the electron escape time was estimated to be approximately 5 ps (see below). This is much less than the electron-scattering time, provided that the electron energy is less than the optical phonon energy, and suggests that electrons escape the SL ballistically, giving rise to the inversion. Note that such a method to maintain inversion is analogous to that used in molecular microwave oscillators.[22] The electron distribution is illustrated in Fig. 6(a), where we show the region of populated states in electron momentum space. Here k_x and k_y are parallel to the layers of the SL and correspond to free in-plane motion, and k_z is normal to the layers and corresponds to the electron motion in the SL periodic potential. The electron distribution is determined by the energy and momentum conservation under the process of photoexcitation,

$$\hbar\Omega = E_g^* + \hbar^2(k_x^2 + k_y^2)(m_e + m_h)/(2m_e m_h) + (\Delta_e + \Delta_h)(1 - \cos k_z d)/2, \quad (1)$$

where the so-called tight-binding model of the electron miniband is assumed,[20] $\hbar\Omega$ is the pumping photon energy, E_g^* is effective gap of the SL; $m_{e,h}$ and $\Delta_{e,h}$ are the effective mass and miniband width for electrons and holes. Since the spectral width of the pump-laser radiation is quite narrow, about 0.5 meV, the populated states are concentrated around the "surface" shown in Fig. 6(a) of "thickness" determined by the mentioned spectral width, or, in other words, dispersion of $\hbar\Omega$. In the particular case of Fig. 6(a), the photon energy $\hbar\Omega$ is chosen such that $\hbar\Omega - E_g^* = 30$ meV, and all photogenerated carriers have nonzero in-plane wave vector. Apparently, such a distribution is characterized by a population inversion. However, such an inversion electron distribution does not necessarily give rise to amplification due to stimulated emission of any phonon mode. This is because electrons may make transitions to empty higher or lower energy states with, respectively, the absorption or emission of a phonon. Each of these processes is controlled by the momentum and energy conservation laws. For amplification of a particular mode to occur, the probability of emission must be greater than the probability of absorption. If this is the case, the population of the mode will become unstable and be

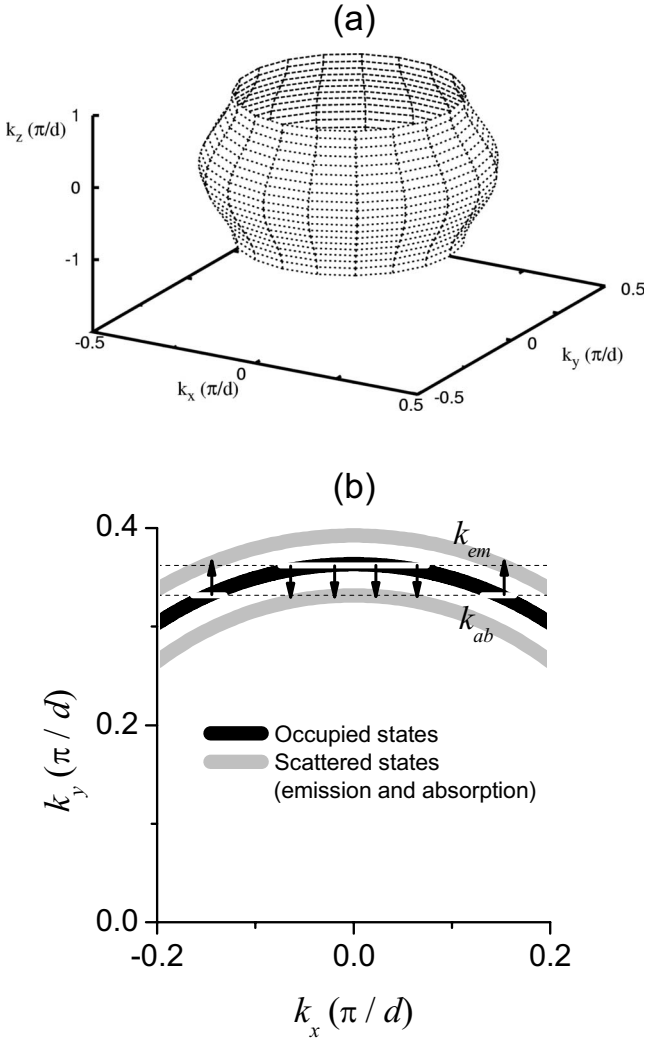

FIG. 6. (a) Electron distribution in the photoexcited SL. (b) Illustration of the feasibility of sound amplification in SL. The black ring represents the populated electron states at particular value of k_z, and the gray rings inside (outside) show scattered electron states with emission (absorption) of a transverse phonon frequency $\omega = 2\pi c_s/d \approx 470$ GHz, and transferring no z component of momentum to electrons. For the lateral component of the phonon wave vector directed along the y axis, the horizontal lines at $k_y = k_{em}, k_{ab}$ mark the possible electron states capable of emitting (absorbing) the phonon, and their white portions show such states which are actually populated. One can see that in this case emission prevails absorption and sound amplification is theoretically possible.

amplified. A qualitative illustration of the feasibility of amplification of a particular mode having frequency $\omega = 2\pi c_s/d$, and for which phonon-assisted electron transitions occur with conservation of k_z, is shown in Fig. 6(b). In this case, the electron transitions are within the planes obtained from the distribution of Fig. 6(a) by cross sections at constant k_z. Due to the isotropic electron dispersion in the x-y plane, in such cross sections the populated electron states are within a ring, part of which is shown in Fig. 6(b) by the black curve. Similarly, the scattered states after the phonon emission (absorption) must be within the rings of smaller (larger) radius. If we assume the phonon in-plane wave vector is directed along the y axis and is of magnitude q, then elementary consideration of the energy and momentum conservation under the electron-phonon scattering process provides that for electrons emitting such a phonon, $k_y = q/2 + m_e\omega/(\hbar q) \equiv k_{em}$, while for electrons absorbing such a phonon $k_y = q/2 - m_e\omega/(\hbar q) \equiv k_{ab}$. A particular case corresponding to relatively small q is shown in Fig. 6(b). According to the wave vector constraint, the emitting electrons are situated on the white portion of k_{em} line, while the absorbing electrons are on the white portions of the k_{ab} line. As can be seen, in this particular case, the number of emitting electrons exceeds the number of absorbing electrons, suggesting amplification of this phonon mode is possible.

It should be mentioned that, in our case, the electron density in the active SL is as low as 10^{21} m^{-3}. It is unlikely that for such density conventional bulklike mechanisms of electron-phonon coupling can provide strong enough amplification of phonons even in the presence of inversion. However, we found recently that, in an SL, the piezoelectric electron-phonon interaction can be enhanced dramatically for particular phonons, which we call *resonant*.[17] These phonons have energy $\hbar\omega$ close to $2\pi\hbar c_s/d$ and are emitted or absorbed at a very small angle θ to the SL normal. For resonant phonons, piezoelectric coupling in the GaAs/AlAs SL can exceed bulklike coupling by more than an order of magnitude,[17] which facilitates achievement of amplification. To determine the theoretical possibility of saser action, it is necessary to analyze rigorously the value of the phonon increment: $\alpha \equiv P_{em} - P_{abs}$, where P_{em} and P_{abs} are, respectively, the probabilities of the phonon emission and absorption. We start first with consideration of the electron contribution to α.

In the tight-binding approximation, the spectrum and wave functions of electrons in a SL are determined as

$$E_e(k_\parallel, k_z) = \frac{\hbar^2 k_\parallel^2}{2m_e} + \frac{\Delta_e}{2}[1 - \cos(k_z d)],$$

$$\psi = \frac{1}{\sqrt{SN}} \exp(ik_x x + ik_y y) \sum_{n=0}^{N-1} \exp(ik_z dn)\chi(z - nd), \quad (2)$$

where S is a normalizing area, N is the number of periods in the SL, and χ is the orbital corresponding to the electron wave function confined in an individual QW. The electron-phonon interaction is determined by the piezoelectric potential, ϕ, induced by the phonon-related strain. The Poisson equation for ϕ is

$$\nabla^2 \phi = \frac{1}{\varepsilon \varepsilon_0} \nabla \cdot \mathbf{P}, \quad (3)$$

where ε is the dielectric permittivity and ε_0 is the absolute dielectric constant. The polarization, $\mathbf{P}$, induced due to the piezoelectric effect has components: $P_i = e_{ijk}(z)u_{jk}$, where u_{jk} is strain tensor and e_{ijk} are piezoconstants, which are different in the QW and barrier layers of the SL. In our case, where elastic mismatch of the layers of the SL has very little effect on its phonon spectrum, it is possible to assume the plane-wave character of the phonon. The periodic z depen-

dence of e gives rise to a complex form of ϕ, which for a phonon of wave vector $\mathbf{q}$ can be presented as a series

$$\phi = -\exp(iq_z z + iq_x x + iq_y y)\sum_{n=-\infty}^{\infty}\frac{R_n \exp(iq_0 nz)}{(q_z+q_0 n)^2+q_\parallel^2}. \quad (4)$$

Here $q_\parallel=\sqrt{q_x^2+q_y^2}$, $q_0=2\pi/d$, and the coefficients R_n are determined by the symmetry of the QW and barrier materials as well as the direction of SL growth (see Ref. 17). The form of the denominator suggests a strong potential for resonant phonons $[(q_z+q_0 n)d, q_\parallel d \ll 1]$, which is a smooth function of z. Note, that a similar resonance also occurs when the actual Bloch-like structure of the SL phonon modes is considered.

Neglecting the overlap of the neighboring orbitals while calculating the matrix element of electron-phonon scattering, we obtain for the probabilities of the phonon emission and absorption the following expression:

$$P_{em,ab} = \frac{(2m_e)^{3/2}}{8\pi^2\rho\omega\hbar^3 q_\parallel} J_{\mathbf{q}} \int d\varepsilon_\parallel dk_z \frac{f(\varepsilon_\parallel,k_z)}{\sqrt{\varepsilon_\parallel - E_{em,ab}}}. \quad (5)$$

Here $\varepsilon_\parallel=\hbar^2(k_x^2+k_y^2)/2m_e$ and f is electron distribution function. The characteristic energies for emission and absorption are $E_{em,ab}=\{E_\parallel \pm \hbar\omega+\Delta_e[\cos k_z d-\cos(k_z \mp q_z)d]/2\}^2/(4E_\parallel)$, where $\hbar\omega$ is the phonon energy and $E_\parallel=\hbar^2 q_\parallel^2/(2m_e)$. The limit of the integral over $\varepsilon_\parallel$ in Eq. (5) is $\varepsilon_\parallel > E_{em,ab}$, which reflects energy and momentum conservation under the phonon emission and absorption processes. In Eq. (5), $J_{\mathbf{q}}$ corresponds to the form factor of the electron-phonon coupling in multiple quantum well structures analyzed in Ref. 17 and determined as

$$J_{\mathbf{q}} = \left|\int \chi^2 \phi dz\right|^2, \quad (6)$$

where normalization of ϕ is selected such that the amplitude of the displacement is unity. As it was shown in Ref. 17, for resonant transverse phonons ($q_z=-q_0+\delta q_z$, $\delta q_z \ll q_0$) of horizontal and vertical polarizations (i.e., having displacement normal or parallel to the plane of the phonon incidence on the SL interfaces, correspondingly) in a (001) GaAs/AlAs SL

$$J^{(TA,h)} \approx 4\frac{e^2\delta e_{14}^2}{\varepsilon^2\varepsilon_0^2 d^2}\frac{q_\parallel^2}{(\delta q_z^2+q_\parallel^2)^2}\sin^2\frac{q_0 d_B}{2}\cos^2 2\phi_{ph},$$

$$J^{(TA,v)} \approx 4\frac{e^2\delta e_{14}^2}{\varepsilon^2\varepsilon_0^2 d^2}\frac{q_\parallel^2}{(\delta q_z^2+q_\parallel^2)^2}\sin^2\frac{q_0 d_B}{2}\sin^2 2\phi_{ph}. \quad (7)$$

Here δe_{14} is the mismatch of the piezoelectric constant in GaAs and AlAs and ϕ_{ph} is the polar angle of the phonon in-plane wave vector. As we see, the coupling of horizontally and vertically polarized transverse phonons can be distinguished only by the dependence on ϕ_{ph}. In the following, we analyze the case of angle ϕ_{ph} for which the increment is maximal.

Under the laser pumping, the distribution function can be approximated as

$$f(k_\parallel,k_z) = \begin{cases} f_0(k_z), & |\hbar\Omega - E_g^* - E_e(k_\parallel,k_z) + E_h(k_\parallel,k_z)| < \delta EM/(2m_e) \\ 0, & \text{otherwise} \end{cases}, \quad (8)$$

where δE is the spectral width of the laser and $M=m_e m_h/(m_e+m_h)$ is the reduced mass. The parameter f_0 can be estimated from the condition of balance of the electron photoexcitation and ballistic escape,

$$f_0 \approx \frac{\pi^2\hbar^2 P_{laser}\xi}{\hbar\Omega k_{\max} M\delta E v_e(k_z)}, \quad (9)$$

where P_{laser} is the laser power density, ξ is the fraction of photons absorbed in SL, and $k_{\max}$ is the maximum value of k_z for states populated by electrons. The characteristic velocity of electron escape, v_e, can be determined from the electron dispersion, Eq. (2), as $v_e=\Delta_e d/(2\hbar)\sin k_z d$. In our case $\Delta_e \approx 10$ meV and $\Delta_e d/(2\hbar)\approx 6\times 10^4$ m/s. Apparently, for $k_z=0, \pi/d$ we get zero escape velocity due to electron Bragg reflection and unphysical divergence of the electron population. In general, for such electrons, removal can be due to scattering. In our case, however, we suppose that faster leakage rate can be provided due to the finite length of the SL, l, which gives to rise to an uncertainty in electron wave vector $\delta k_z \sim 2\pi/l$. According to this estimate, in our further calculations we restricted the minimal value of v_e: $v_e > \pi\Delta_e d/(N\hbar)$, where N is the number of periods in the active SL.

Analysis of the increment in the general case is a complicated problem. However, it is easy to consider a particular case of $\delta q_z=0$. In this case $E_{em,ab}$ do not depend on k_z and $E_{em}=E_{ab}+\hbar\omega$. Figure 7(a) shows the populated electron states by the shaded region in k_z-$\varepsilon_\parallel$ plane. We show also by the horizontal lines E_{em} and E_{ab} for two values of $q_\parallel$. In the case corresponding to the superscript (1) both phonon emission and absorption are possible for any k_z. However, the form of expression (5) suggests that the probability of emission exceeds that of absorption and the increment is positive. In case (2) only absorption is possible, and the increment is negative. Figure 7(b) shows the dependence of $E_{em,ab}$ on $q_\parallel$ for resonant phonons. As we see the dependence is very sharp in the region of small $q_\parallel$. This means that very small variation in $q_\parallel$ changes the increment significantly.

The results of numerical calculations for α are shown in Fig. 8 for the pumping power of 2 kW cm^{-2}, $\hbar\Omega - E_g^* = 30$ meV, the materials parameters used are given in Ref.

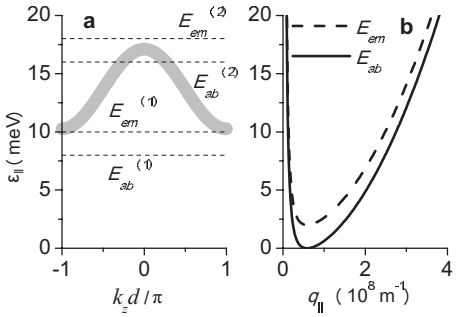

FIG. 7. Illustration of the electron population inversion (a). The shaded area marks the region of electron in-plane energy and k_z where the electron distribution function is concentrated. The characteristic energies $E_{em,ab}$ are marked for two particular values of $q_{\|}$ and $\delta q_z=0$. (b) The dependence of $E_{em,ab}$ on $q_{\|}$ for resonant phonons.

23, and $\xi=0.49$ (the latter value assumes 30% reflection of light from the sample surface and 70% absorption within the active SL). In our case we do not know the exact value of δE. Experimentally, it was determined to be, in any case, less than 0.5 meV. Due to this uncertainty, we show results of for the increment for the two different values of δE, 0.5 and 0.1 meV, in Figs. 8(a) and 8(b), respectively. We see, that in accordance with the above analysis, in very narrow range of in-plane phonon wave vectors α is positive and has large magnitude.

The contribution of the photogenerated holes to the increment can be calculated in a way similar to that of electrons. The important point here is feasibility of hole inversion. In our case we calculated the heavy-hole miniband width to be

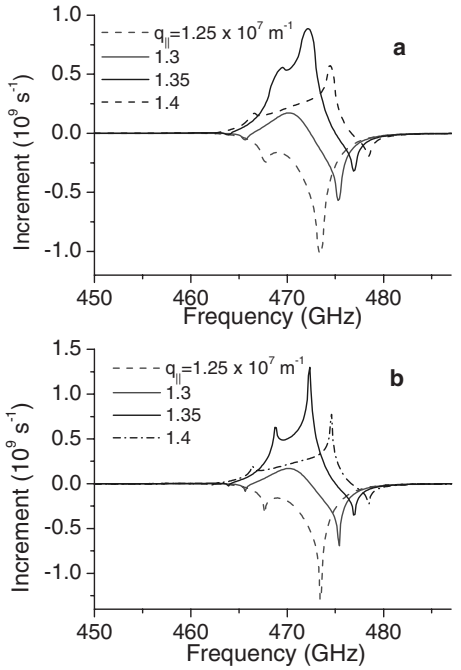

FIG. 8. Numerical results for the electron contribution to the phonon increment for different values of the in-plane phonon wave vector. The cases (a) and (b) correspond to the spectral width of the pumping laser radiation 0.5 and 0.1 meV, respectively.

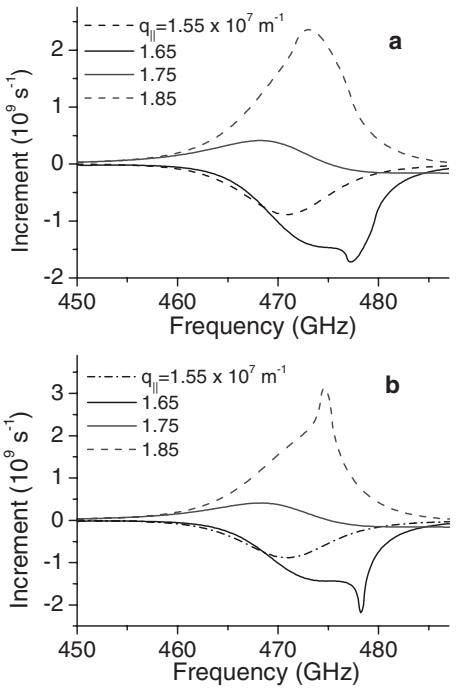

FIG. 9. As Fig. 8 but for the hole contribution to the increment.

$\Delta_h \approx 2$ meV, and the characteristic escape time about 25 ps. This time is short enough to provide ballistic escape of holes. For this case the results for the hole contribution to the increment are provided in Fig. 9. As we see, it is greater than that of electrons, which is a direct result of slower escape of holes and their stronger accumulation in the active SL. Due to different values of the lateral effective masses of electrons and holes, they provide large value of increment to the phonons of slightly different lateral wave vectors. Note, that for the wave vectors corresponding to the large electron increment shown in Fig. 8, the contribution of holes is negative, giving rise to considerable decrease in increment. On the other hand, electron contribution to the increment in the range of lateral wave vectors corresponding to Fig. 9 is small. This suggests that provided that the hole inversion exists in the system, stimulated phonon emission is mainly due to their coupling with holes. However, we have to mention here that fluctuation of the thicknesses of the layers of the SL can give rise to localization of holes, which leads to their thermalization. Since thermalized holes do not interact with the phonons of interest due to energy and momentum conservation, the phonon emission in this case would be due to electrons. Unfortunately we cannot be certain in our particular case on the ballistic character of hole removal from the active SL and to conclude weather electrons or holes provide the major contribution to stimulated phonon emission.

To estimate the feasibility of stimulated emission, we have to take into account finite quality factor of the phonon cavity. Consider the active SL of length l within a Fabry-Pérot cavity of length L between a SL Bragg mirror, reflectivity R_m, and the top surface of the structure, reflectivity R_s. Using the same analysis as for a laser (see, e.g., Ref. 24), the round-trip gain is given by

$$G = R_m R_s \exp\left\{2\left(\frac{\alpha l}{c_s} - \frac{L}{\bar{\ell}}\right)\right\},$$

where c_s is the velocity of transverse sound and $\bar{\ell}$ is the phonon mean free path. The first term in the brackets accounts for growth of the acoustic intensity due to amplification and the second term accounts for losses due to scattering in the cavity. The threshold condition for saser oscillation to occur is $G=1$, giving

$$\alpha_{th} = \frac{c_s}{l}\left\{\frac{L}{\bar{\ell}} + \frac{1}{2}\ln\left(\frac{1}{R_m R_s}\right)\right\}. \quad (10)$$

Substituting the values for our structure: $c_s=3500$ ms^{-1}; $l=0.3$ μm; $L=1$ μm; $\bar{\ell}=0.8$ mm (Ref. 25); $R_s=0.8$ (Ref. 26); and $R_m \sim 1$, gives $\alpha_{th} \approx 1\times 10^9$ s^{-1}. Therefore saser oscillation is theoretically possible for pumping at less than 2 kW cm^{-2}. This is in a reasonable agreement with the experimental observation of a threshold at about 0.5 kW cm^{-2}.

We have to note that, in our case, phonon generation is not steady state, at least in some interval of pumping power around threshold. This conclusion can be drawn immediately by comparison of the predicted increment and inverse duration of the pumping pulse, T^{-1}. Experimental evidence is provided by the character of the dependence of the phonon signal on the pumping power. If no nonlinear process responsible for saturation of the phonon radiation power in steady state is present, then the bolometer signal is proportional to $\exp[(\alpha-\alpha_{th})Tl/L]$, where α scales linearly with P_{laser}. In Fig. 10 we plot the power dependence of the bolometer signal on P_{laser} for $\lambda=750$ nm. From this graph exponential dependence is clearly seen. From the slope of this dependence and bearing in mind the threshold power value about 0.5 kW/cm^2 we obtain $\alpha_{th} \approx 2\times 10^8$ s^{-1}. Taking into account the rough character of the model used we think this number is in a reasonable agreement with the theoretical estimate given above. Finally, we should mention also that in non steady-state regime we deal with multimode stimulated emission with relatively low degree of coherence.

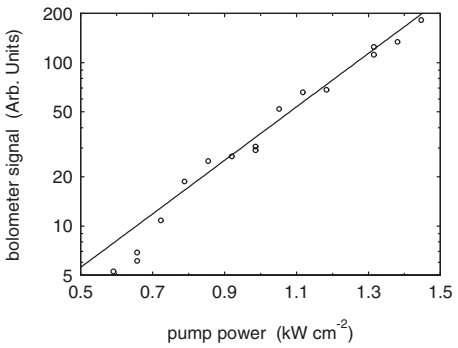

FIG. 10. Bolometer signal with the extrapolated linear below-threshold contribution subtracted as a function of the pump power density (data points). The exponential character of the power dependence is clearly seen in the fit to the experimental data (line).

V. CONCLUSIONS

In conclusion, we have observed experimental evidence of saser action in the emission of terahertz transverse phonons from a GaAs/AlAs superlattice under interband optical pumping. The primary evidence for saser action was a strong increase in the TA emission in a direction normal to the SL layers when pumping above the threshold intensity. We have shown that the important conditions for saser operation are met in our device structure: formation of an inversion charge-carrier distribution in the optically pumped SL; resonantly enhanced piezoelectric electron-phonon coupling for phonons propagating close to the SL axis; and realization of a Fabry-Pérot phonon cavity. Such a source of monochromatic nanometre-wavelength sound could potentially be used for acoustic spectroscopy and imaging of nanoscale materials and structures.

ACKNOWLEDGMENTS

This work was supported by the Royal Society of the UK. B.A.G. and V.A.K. were also supported by STCU through Grant No. 3922.

[1] P. Hawker, A. J. Kent, and M. Henini, Physica B **263-264**, 514 (1999).
[2] A. Yamamoto, T. Mishina, Y. Masumoto, and M. Nakayama, Phys. Rev. Lett. **73**, 740 (1994).
[3] A. Bartels, T. Dekorsy, H. Kurz, and K. Kohler, Phys. Rev. Lett. **82**, 1044 (1999).
[4] C.-K. Sun, J.-C. Liang, and X.-Y. Yu, Phys. Rev. Lett. **84**, 179 (2000).
[5] E. Makarona, B. Daly, J.-S. Im, H. Maris, A. Nurmikko, and J. Han, Appl. Phys. Lett. **81**, 2791 (2002).
[6] M. Trigo, T. A. Eckhause, J. K. Wahlstrand, R. Merlin, M. Reason, and R. S. Goldman, Appl. Phys. Lett. **91**, 023115 (2007).
[7] K.-H. Lin, C.-M. Lai, C.-C. Pan, J.-I. Chyi, J.-W. Shi, S.-Z. Sun, C.-F. Chang, and C.-K. Sun, Nat. Nanotechnol. **2**, 704 (2007).
[8] D. Hofstetter and J. Faist, in *Solid-State Mid-Infrared Laser Sources*, edited by I. T. Sorokina and K. L. Vodpyanov (Springer, Berlin, 2003).
[9] W. Liang, K. T. Tsen, O. F. Sankey, S. M. Komirenko, K. W. Kim, and V. A. Kochelap, Appl. Phys. Lett. **82**, 1968 (2003).
[10] S. S. Makler, M. I. Vasilevsky, E. V. Anda, D. E. Tuyarot, J. Weberszpil, and H. M. Pastawski, J. Phys.: Condens. Matter **10**, 5905 (1998).
[11] B. A. Glavin, V. A. Kochelap, and T. L. Linnik, Appl. Phys. Lett. **74**, 3525 (1999).
[12] S. M. Komirenko, K. W. Kim, A. A. Demidenko, V. A. Kochelap, and M. A. Stroscio, Phys. Rev. B **62**, 7459 (2000).
[13] L. G. Tilstra, A. F. M. Arts, and H. W. de Wijn, Phys. Rev. B **76**, 024302 (2007).
[14] A. J. Kent, R. N. Kini, N. M. Stanton, M. Henini, B. A. Glavin, V. A. Kochelap, and T. L. Linnik, Phys. Rev. Lett. **96**, 215504

(2006).
[15] G. P. Srivastava, *The Physics of Phonons* (A. Hilger, Bristol, 1990).
[16] M. F. Pascual Winter, G. Rozas, A. Fainstein, B. Jusserand, B. Perrin, A. Huynh, P. O. Vaccaro, and S. Saravanan, Phys. Rev. Lett. **98**, 265501 (2007).
[17] B. A. Glavin, V. A. Kochelap, T. L. Linnik, A. J. Kent, N. M. Stanton, and M. Henini, Phys. Rev. B **74**, 165317 (2006).
[18] M. N. Wybourne and J. K. Wigmore, Rep. Prog. Phys. **51**, 923 (1988).
[19] M. E. Msall and J. P. Wolfe, Phys. Rev. B **65**, 195205 (2002).
[20] J. P. Wolfe, *Imaging Phonons: Acoustic Wave Propagation in Solids* (Cambridge University Press, Cambridge, England, 1998).
[21] *Semiconductor Superlattices: Growth and Electronic Properties*, edited by H. T. Grahn (World Scientific, Singapore, 1995).
[22] J. P. Gordon, H. J. Zeiger, and C. H. Townes, Phys. Rev. **95**, 282 (1954).
[23] *Handbook Series on Semiconductor Parameters*, edited by M. Levinstein, S. Rumyantsev, and M. Shur (World Scientific, London, 1999), Vol. 2.
[24] F. G. Smith, T. A. King, and D. Wilkins, *Optics and Photonics: An Introduction*, 2nd ed. (Wiley, Chichester, 2007).
[25] A. J. Kent, N. M. Stanton, L. J. Challis, and M. Henini, Appl. Phys. Lett. **81**, 3497 (2002).
[26] G. A. Northrop and J. P. Wolfe, Phys. Rev. Lett. **52**, 2156 (1984).